Remote Sensing Letters
April 2022, Volume 13 Issue 4 Pages 334-342
https://doi.org/10.1080/2150704X.2022.2032452
https://archimer.ifremer.fr/doc/00750/86183/

Eastward propagating surface salinity anomalies in the tropical North Atlantic

Grodsky Semyon A. [1,*], Reul Nicolas [2], Bentamy Abderrahim [2], Vandemark Douglas [3]

[1] Department of Atmospheric and Oceanic Science, University of Maryland, College Park, MD, USA
[2] Laboratoire d'Océanographie Physique et Spatial (LOPS), Institut Francais Pour la Recherche et l'Exploitation de la Mer, Plouzané, France
[3] Ocean Process Analysis Laboratory, University of New Hampshire, Durham, NH, USA

* Corresponding author : Semyon A. Grodsky, email address : senya@atmos.umd.edu

Abstract :

Upper ocean variations across the tropical Atlantic are strongly seasonal due to corresponding seasonality in surface forcing and continental runoff. This implies that many features in regional upper ocean state or transport anomalies may also be seasonally locked. In the boreal summer and autumn, remote sensing sea surface salinity (SSS) observations show the presence of eastward propagating anomalies concurrent with the seasonal development of fresh Amazon plume and acceleration of the eastward North Equatorial Countercurrent. Interannual variations in these eastward cross-Atlantic SSS signals are investigated in connection with their forcing by wind and circulation patterns. Satellite data show that these SSS anomalies are advected zonally across the entire Atlantic. It is suggested that they originate due to wind-induced changes in the Amazon plume areal extent, which are notorious in the North Brazil Current retroflection. Satellite SSS is instrumental for exploring such signals because in-situ observations do not always capture them due to the limitation in resolved spatial and temporal scales.

1 Introduction

Meridional migration of the Intertropical Convergence Zone (ITCZ) between its southernmost position in boreal spring and northernmost position in late boreal summer defines the strong seasonality of tropical Atlantic climate (Xie and Carton 2013). This implies that major interannual modes of regional sea surface temperature (SST) variability driven by local air-sea interactions (Foltz et al. 2003) are also seasonally locked, including the Atlantic Meridional Mode peaking in boreal spring e.g., (Nobre and Srukla 1996) and the Atlantic Zonal Mode peaking in boreal summer (e.g., Zebiak 1993). Like the SST, the sea surface salinity (SSS) is also governed by meridional shifts of the ITCZ and its impacts on ocean surface fluxes and continental runoff (Lentz 1995). But in contrast to SST that can be more rapidly altered by air-sea interactions, upper ocean salinity undergoes less change and provides a clearer tracer for oceanic advection (Foltz et al. 2004), thus allowing the study of surface transport over larger distances in this tropical basin.

Tropical Atlantic SSS distribution includes a zonal band of relatively low SSS that is formed between 10°S-15°N due to the seasonally shifting ITCZ. It also includes a fresh SSS plume formed by Amazon discharge (peaking in mid-May and decreasing to its seasonal minimum in mid-November) that spreads over an area of 10^6 km^2 by early boreal autumn (Dessier and Donguy 1994). The interannual variability of the plume area is controlled by multiple factors, with Amazon runoff variations accounting for ~50% (Zeng et al., 2008). But other factors, including cross-shore winds that modify offshore plume dispersal (Molleri, Novo, and Kampel 2010); (Fournier et al. 2017), regional western boundary current variability (Grodsky et al. 2014); (Grodsky, Carton, and Bryan 2014), as well as Pacific teleconnections (Grodsky and Carton 2018) all contribute. The fresh plume water is advected eastward by the North Equatorial Countercurrent, NECC, (e.g., Carton and Katz 1990), and northwestward along the western boundary towards the Caribbean and Lesser Antilles (Hellweger and Gordon 2002). In August – October, about 70% of the Amazon plume water turns eastward in the NECC along the North Brazil Current (NBC) retroflection (Lentz 1995).

The eastward NECC is a possible gateway for zonal salinity anomaly propagation. In contrast to the more commonly observed wave-induced westward anomaly propagation by the Rossby waves (Killworth, Chelton, and de Szoeke 1997), eastward propagating anomalies have also been detected in major eastward currents, e.g., on poleward flanks of subtropical gyres (Taguchi and Schneider 2014). Here, most of the attention was paid to density compensated subsurface anomalies advected eastward at thermocline depths (Sasaki et al. 2010). Besides this subsurface regime, mixed layer anomalies may remain surface trapped (thus exposed to the remote sensing) and then advected by local surface currents for a prolonged period of weeks to months, with positive buoyancy supported by the stably stratified thermocline below the mixed layer. Eastward SSS propagation is also evident in the tropical Indian Ocean during negative dipole events (Sun et al. 2019) with an interruption during El Nino-induced westward current reversals (Grodsky, Carton, and Murtugudde 2001). The tropical north Atlantic is an ideal system for observing such surface trapped eastward salinity anomalies produced by highly variable western boundary current dynamics that impact Amazon plume water and its export into the eastward NECC via the NBC retroflection.

Until recently, most information on tropical Atlantic SSS change has come from in situ measurements. In the last decade, traditional in-situ salinity measurements have been augmented by SSS measurements from three microwave satellite L-band (1.4 GHz) instruments (e.g., Reul et al. 2020). Here we exploit the Soil Moisture Active Passive (SMAP, since 2015) (Meissner et al. 2019) satellite data to show that SSS anomalies originating in the tropical northwestern Atlantic can be advected by the NECC across the entire Atlantic towards the African coast. Satellite SSS data are instrumental for exploring such eastward propagating salinity signals because in-situ measurements (e.g., the Prediction and Researched Moored Array in the Atlantic, PIRATA, and Argo profiling floats) do not always capture them due to the limitation in resolved spatial and temporal scales.

2 Results

Figure 1 illustrates the August climatological distribution of tropical Atlantic SMAP SSS and geostrophic zonal currents from the Archiving, Validation and Interpretation of Satellite Oceanographic data (AVISO) multi-satellite merged altimetry (http://marine.copernicus.eu). The Amazon freshwater plume configuration, with SSS≤35 psu, reflects the Amazon runoff entering the ocean at approximately 0°N and its transport northwestward along the western boundary (Hellweger and Gordon 2002). Importantly, a connected area of relatively fresh 33< SSS <35 psu also extends eastward along the NECC (between 4°N−10°N and 30°W−44°W). This surface water reflects the combined impact of ITCZ rainfall and eastward Amazon plume advection. But in contrast with the August climatological ITCZ rainfall that is stronger east of 40ºW (not shown), this fresh SSS distribution is weighted towards the west (Figure 1) consistent with the expected impact of freshwater advection from the plume (e.g., Foltz et al. 2004).

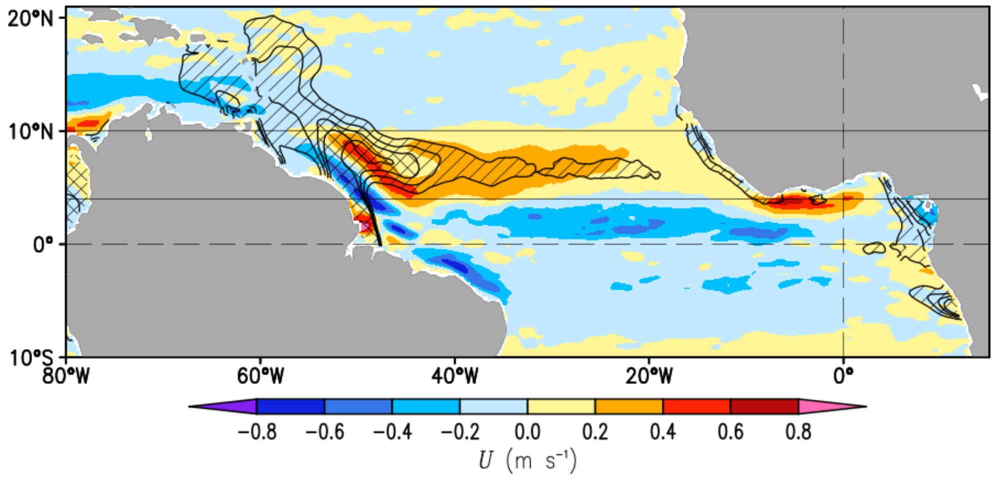

Figure 1. August climatological zonal geostrophic velocity (*U*, shaded, positive - eastward) and sea surface salinity (SSS) contoured at 32, 33, 34, and 35 psu. SSS≤33 psu is cross-hatched and 33<SSS<=35 psu is hatched. The latitudinal range (4°N−10°N) of the eastward North Equatorial Countercurrent, NECC, is delineated by solid lines.

Examining SSS variability within the zonal NECC belt across 4°N−10°N (Figure 2a) reveals an eastward propagation in satellite SSS anomalies (SSSA; defined as the deviation from the monthly seasonal SSS cycle), with SSSA signals of ~0.5 psu crossing the entire tropical Atlantic. They develop seasonally along with the NECC, originate in the west by late spring to early summer, and cross the Atlantic by year-end. Figure 2 illustrates their kinematics and potential forcing terms. These eastward salinity signals are not likely forced by local air-sea interactions, as illustrated by Evaporation-minus-Precipitation, EmP, anomalies from the fifth generation of the European Centre for Medium-Range Weather Forecasts atmospheric reanalysis (ERA5, Hersbach et al. 2020), which do not seem to display a similar eastward propagation (Figure 2b). Their characteristic propagation speed ~0.2 m s^{-1} (Figure 2a) corresponds to the NECC zonal geostrophic velocity (Figure 2c). But, NECC acceleration events observed in 2017 and 2018 (Figure 2c) correspond to two opposite sign salinity events with fresh and salty NECC states (Figure 2a), respectively. This, in turn, suggests that SSS anomalies exiting the plume area via the NBC retroflection are further advected eastward by the mean NECC current ($\bar{u}S'$ transport term) while the salinity transport component by anomalous zonal velocity ($u'\bar{S}$ transport term) is not at play, where overbar is the mean and prime is the anomaly.

It is anticipated that the Amazon runoff anomaly may also contribute. But only in 2016 can the saltier NECC state be linked to preceding below-normal Amazon runoff (Figure 2d, runoff data from the Amazon basin water resources observation service, https://hybam.obsmip.fr/). During other years, the sign of SSS anomaly does not correlate with the sign of Amazon runoff anomaly. Amazon runoff anomalies are not coincident with the runoff peak in May but are rather associated with changes in its annual phase and duration (Figure 2d).

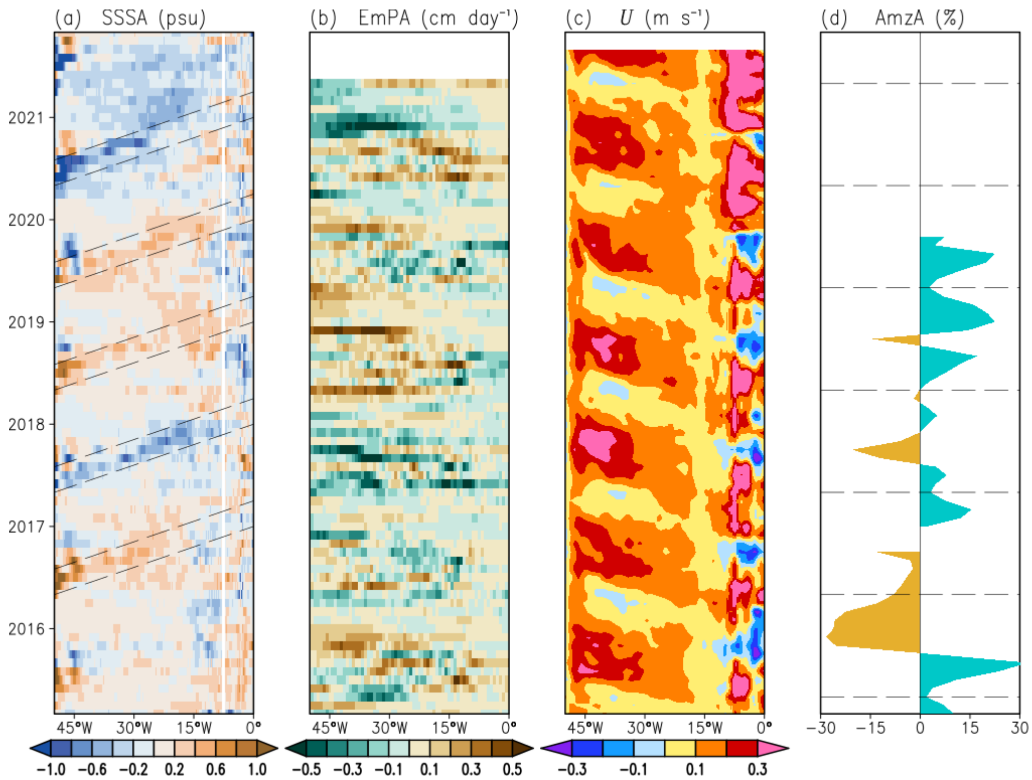

Figure 2. Monthly mean 4º-10ºN averages of (a) sea surface salinity anomaly (SSSA), (b) Evaporation-minus-Precipitation anomaly (EmPA), (c) total zonal geostrophic velocity (U), and (d) relative anomaly (AmzA $= (R - R_s)/R_s$) of Amazon runoff (R) from its seasonal cycle (R_s). Horizontal lines in (d) are drawn 1-st of May each year when Amazon runoff maximizes. Diagonal lines in (a) show 25 cm s^{-1} propagation speed.

Regardless of their cross-Atlantic zonal extent (see longitude-time diagrams in Figure 2a), the eastward SSSA signals have a smaller meridional size and are not firmly captured by the existing in-situ observing systems, which do not always sample them due to the limitation in resolved spatial and temporal scales. As an example, Figures 3a and 3b show spatial patterns of fresh SSSA observed by the SMAP during two sample months of 2017. In November 2017, the Argo float network (Figure 3d) captures reasonably well the fresh SMAP-observed SSSA pattern located at ~20ºW (Figure 3b). But there is a large discrepancy in September 2017 where the Argo zonal salinity anomaly data (Figure 3c) grossly mispresent regional satellite-observed SSS variations. When captured, the gridded Argo analysis does represent the expected vertical characteristics associated with these eastward SSSA signals, increasing from ~20 m to ~40 m as they propagate from the west into the tropical eastern Atlantic (Figures 3c, 3d). In the west and close to the plume, their vertical scale corresponds to the vertical scale of barrier layers in the plume, ~20 m (e.g., Liu, Grodsky, and Carton 2009). In the east, it deepens to ~ 40 m that may be interpreted as a result of the vertical diffusion of salinity anomalies as they are advected eastward by the NECC and propagate away from the Amazon plume.

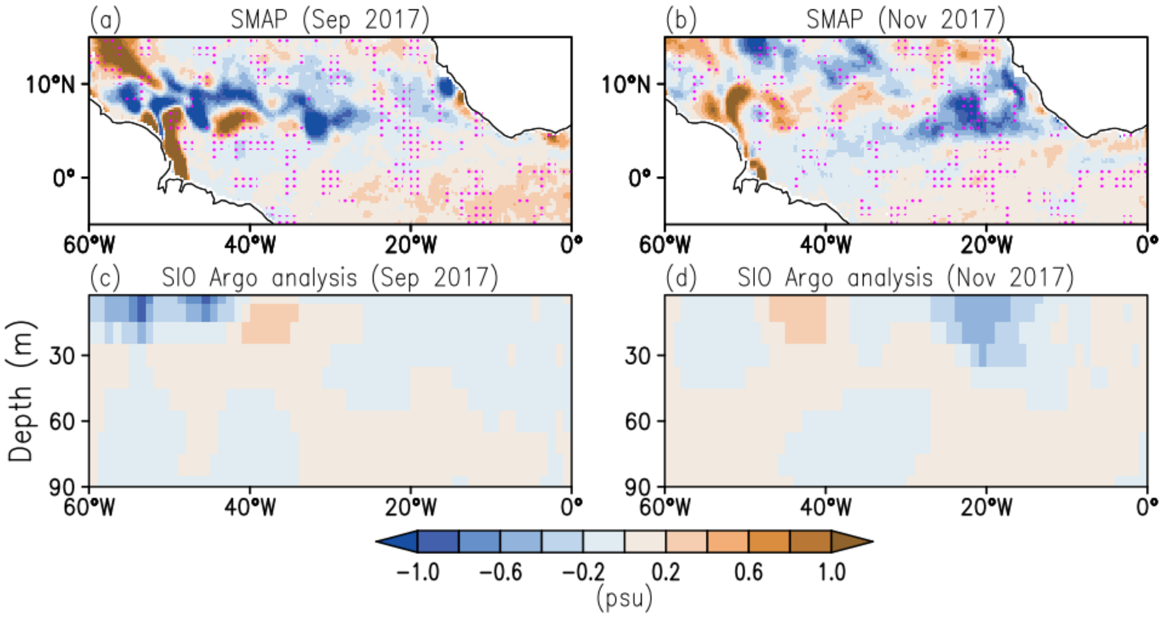

Figure 3. Sample SMAP satellite monthly SSS anomaly (shaded) for (a) September 2017 and (b) November 2017 with Argo data coverage hatched by purple dots. (c, d) Corresponding Argo depth-longitude salinity anomaly averaged 4°N-10°N from the Scripps Institute of Oceanography analysis (Roemmich and Gilson 2009).

From the above considerations, it remains uncertain which mechanisms may be responsible for variability observed in eastward SSSA signals carried in the NECC in this time period each year. As mentioned, the 2016 SSSA increase may be related to a decrease in corresponding Amazon runoff in preceding months (Figure 2). But other years do not show this plausible forcing relationship. This is not surprising because the year-to-year plume variability is also affected by the variability of ocean currents (Grodsky et al. 2014).

Previous research has hypothesized that the strength of cross-shore winds over the tropical northwestern Atlantic can regulate the cross-shore plume extent by modifying its dispersal by mesoscale currents (Molleri, Novo, and Kampel 2010). Such indirect wind-induced changes of plume extent, in turn, modify the salinity of the water that enters the NECC through the NBC retroflection. Examining gridded satellite Advanced Scatterometer (ASCAT) winds (Bentamy and Fillon 2012) during months (May-July) corresponding to the annual development of salinity anomalies in the western NECC for years with fresh (Figures 4a, 4b) and salty

(Figures 4c, 4d) NECC states supports the above hypothesis. In 2017 and 2020, the wind anomalies were offshore (Figure 2a). This favored Amazon plume dispersal off the shelf and allowed for fresher water to be retroflected into the western NECC, which was further advected eastward. Conversely, May-July wind anomalies in 2018 and 2019 were onshore. This appears to lessen the plume area and place it nearer to the coast, ultimately resulting in anomalous salinification of the western NECC. Figure 4 also illustrates that changes in the strength of cross-shore winds are related to larger-scale changes in northeasterly trade winds, in turn, linked to the meridional-mode-like SST patterns (Fournier et al. 2017), with weaker winds corresponding to warmer tropical North Atlantic SST and vice versa.

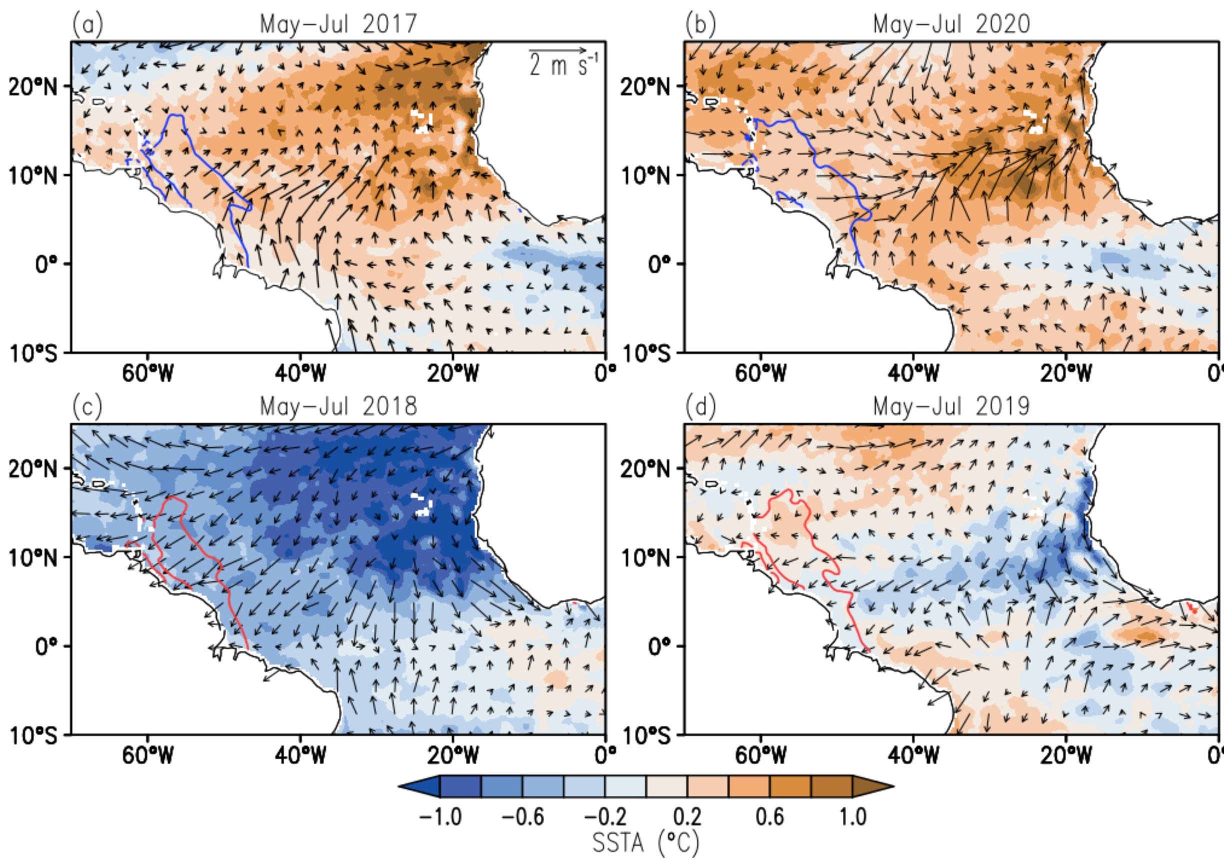

Figure 4. (shaded) Sea surface temperature anomaly (SSTA), (arrows) scatterometer surface wind anomaly, and (solid lines) SSS=34 psu contours during May-July period of years with (a, b) fresh and (c, d) salty NECC states. SSS contour color is (top row) blue (bottom row) red for better contrast with SSTA shading.

From Figure 4, the potential impact of opposing cross-shore wind anomalies on the plume extent is not clearly visible. In Figure 5, Amazon plume extent composites are compared using satellite SMAP SSS separately for years of salty (2016, 2018, and 2019) and fresh (2017 and 2020) NECC states (see also Figure 2a). Even given the limited statistics available from only

5 full years of SMAP data, this comparison illustrates that the plume area contracts somewhat during years of stronger onshore winds, which corresponds to the salty NECC state. The strongest plume contraction is present in the retroflection area and this implies less Amazon freshwater transport into the western NECC during anomalously onshore May-July wind conditions. Variations in this freshwater transport are a key factor of upper ocean salinity variability in the tropical northwestern Atlantic (Foltz et al. 2004).

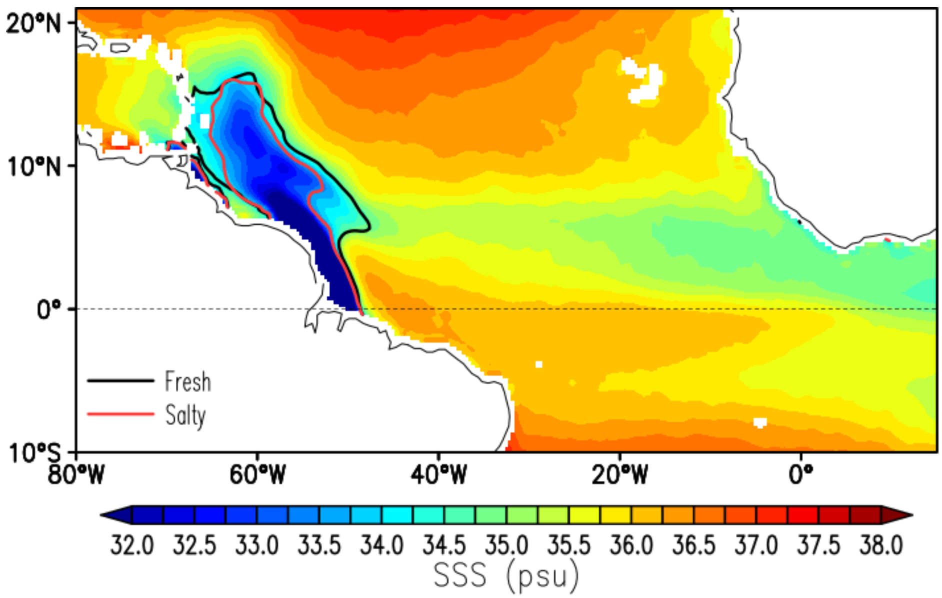

Figure 5. May-July climatological SSS (shaded) with SSS=34 psu contour (solid lines) for years of fresh (2017 and 2020, black) and salty (2016, 2018, and 2019, red) state in the NECC.

3 Summary

SMAP satellite SSS data reveal eastward advective propagation of ~0.5 psu SSS anomalies that cross the entire tropical Atlantic within the North Equatorial Countercurrent (NECC) belt between 4°N and 10°N. They develop seasonally along with the seasonal acceleration of the NECC, originate in the west by late spring to early summer, and reach the eastern tropical Atlantic by year-end. Their characteristic propagation speed (~0.2 m s^{-1}) corresponds to the NECC zonal geostrophic velocity. These salinity anomalies produce year-to-year changes of SSS in the NECC belt, with alternating years of salty and fresh states.

During six years of SMAP SSS observations, only the 2016 salty NECC anomaly may be attributed to the lack of Amazon runoff, while other years do not show this expected relationship. Instead, the sign of NECC salinity anomalies is consistent with the strength of cross-shore winds over the tropical northwestern Atlantic that regulates the cross-shore plume extent by modifying its dispersal by mesoscale currents. Such indirect wind-induced changes of plume extent, in turn, modify the salinity of the water that enters the western NECC through the NBC retroflection and is further advected eastward. Examining scatterometer winds during months (May-July) corresponding to the annual development of salinity anomalies in the western NECC confirms the presence of below normal and above normal onshore wind velocity anomalies during years of fresh and salty NECC states, respectively. Given documented impacts of the Pacific teleconnection on interannual tropical Atlantic SSS (Grodsky and Carton 2018), including the plume, this remote impact cannot be ruled out. But, it is hard to examine much about the Pacific teleconnection with this limited number of SMAP observation years.

Satellite salinity measurements are instrumental for exploring these eastward propagating salinity signals because in-situ measurements do not always capture them due to the limitation in resolved spatial and temporal scales.

Acknowledgments. This research was supported by the NASA Physical Oceanography and Ocean Surface Salinity Teams.

References

Bentamy, Abderrahim, and Denis Croize Fillon. 2012. "Gridded Surface Wind Fields from Metop/ASCAT Measurements." *International Journal of Remote Sensing* 33 (6): 1729–1754. doi:10.1080/01431161.2011.600348.

Carton, J. A., and E. J. Katz. 1990. "Estimates of the Zonal Slope and Seasonal Transport of the Atlantic North Equatorial Countercurrent." *Journal of Geophysical Research* 95 (C3): 3091–3100. doi:10.1029/JC095iC03p03091.

Dessier, Alain, and Jean René Donguy. 1994. "The Sea Surface Salinity in the Tropical Atlantic between 10°S and 30°N—Seasonal and Interannual Variations (1977–1989)." *Deep Sea Research Part I: Oceanographic Research Papers* 41 (1): 81–100. doi:10.1016/0967-0637(94)90027-2.

Foltz, Gregory R., Semyon A. Grodsky, James A. Carton, and Michael J. McPhaden. 2003. "Seasonal Mixed Layer Heat Budget of the Tropical Atlantic Ocean." *Journal of Geophysical Research* 108 (C5): 3146. doi:10.1029/2002JC001584.

Foltz, Gregory R., Semyon A. Grodsky, James A. Carton, and Michael J. McPhaden. 2004. "Seasonal Salt Budget of the Northwestern Tropical Atlantic Ocean along 38°W." *Journal of Geophysical Research: Oceans* 109 (C3): C03052. doi:10.1029/2003JC002111.

Fournier, S, D Vandemark, L Gaultier, T Lee, B Jonsson, and M M Gierach. 2017. "Interannual Variation in Offshore Advection of Amazon-Orinoco Plume Waters: Observations, Forcing Mechanisms, and Impacts." *Journal of Geophysical Research: Oceans* 122 (11): 8966–8982. doi:https://doi.org/10.1002/2017JC013103.

Grodsky, Semyon A., and James A. Carton. 2018. "Delayed and Quasi-Synchronous Response of Tropical Atlantic Surface Salinity to Rainfall." *Journal of Geophysical Research: Oceans* 123 (8): 5971–5985. doi:10.1029/2018JC013915.

Grodsky, Semyon A., James A. Carton, and Frank O. Bryan. 2014. "A Curious Local Surface Salinity Maximum in the Northwestern Tropical Atlantic." *Journal of Geophysical Research: Oceans* 119 (1): 484–495. doi:10.1002/2013JC009450.

Grodsky, Semyon A., James A. Carton, and Raghu Murtugudde. 2001. "Anomalous Surface Currents in the Tropical Indian Ocean." *Geophysical Research Letters* 28 (22): 4207–4210. doi:10.1029/2001GL013592.

Grodsky, Semyon A., Gilles Reverdin, James A. Carton, and Victoria J. Coles. 2014. "Year-to-Year Salinity Changes in the Amazon Plume: Contrasting 2011 and 2012 Aquarius/SACD and SMOS Satellite Data." *Remote Sensing of Environment* 140 (January): 14–22. doi:10.1016/j.rse.2013.08.033.

Hellweger, Ferdi L., and Arnold L. Gordon. 2002. "Tracing Amazon River Water into the Caribbean Sea." *Journal of Marine Research* 60 (4): 537–549. doi:10.1357/002224002762324202.

Hersbach, Hans, Bill Bell, Paul Berrisford, Shoji Hirahara, András Horányi, Joaquín Muñoz-Sabater, Julien Nicolas, et al. 2020. "The ERA5 Global Reanalysis." *Quarterly Journal of the Royal Meteorological Society* 146 (730): 1999–2049. doi:10.1002/qj.3803.

Killworth, Peter D., Dudley B. Chelton, and Roland A. de Szoeke. 1997. "The Speed of Observed and Theoretical Long Extratropical Planetary Waves." *Journal of Physical Oceanography* 27 (9): 1946–1966. doi:10.1175/1520-0485(1997)027<1946:TSOOAT>2.0.CO;2.

Lentz, Steven J. 1995. "Seasonal Variations in the Horizontal Structure of the Amazon Plume Inferred from Historical Hydrographic Data." *Journal of Geophysical Research: Oceans* 100 (C2): 2391–2400. doi:https://doi.org/10.1029/94JC01847.

Liu, Hailong, Semyon A. Grodsky, and James A. Carton. 2009. "Observed Subseasonal Variability of Oceanic Barrier and Compensated Layers." *Journal of Climate* 22 (22): 6104–6119. doi:10.1175/2009JCLI2974.1.

Meissner, T., Wentz, F. J., Manaster, A., Lindsley, R. 2019. "Remote Sensing Systems SMAP Ocean Surface Salinities [Level 2C, Level 3 Running 8-Day, Level 3 Monthly], Version 4.0 Validated Release." Santa Rosa, CA, USA. doi:0.5067/SMP40-3SMCS.

Molleri, Gustavo S.F., Evlyn M.L.de M Novo, and Milton Kampel. 2010. "Space-Time Variability of the Amazon River Plume Based on Satellite Ocean Color." *Continental Shelf Research* 30 (3–4): 342–352. doi:10.1016/j.csr.2009.11.015.

Nobre, Paulo, and J. Srukla. 1996. "Variations of Sea Surface Temperature, Wind Stress, and Rainfall over the Tropical Atlantic and South America." *Journal of Climate* 9 (10). Boston MA, USA: American Meteorological Society: 2464–2479. doi:10.1175/1520-0442(1996)009<2464:VOSSTW>2.0.CO;2.

Reul, N., S.A. Grodsky, M. Arias, J. Boutin, R. Catany, B. Chapron, F. D'Amico, et al. 2020. "Sea Surface Salinity Estimates from Spaceborne L-Band Radiometers: An Overview of the First Decade of Observation (2010–2019)." *Remote Sensing of Environment* 242 (June). Elsevier: 111769. doi:10.1016/j.rse.2020.111769.

Roemmich, Dean, and John Gilson. 2009. "The 2004–2008 Mean and Annual Cycle of Temperature, Salinity, and Steric Height in the Global Ocean from the Argo Program." *Progress in Oceanography* 82 (2): 81–100. doi:10.1016/j.pocean.2009.03.004.

Sasaki, Yoshi N., Niklas Schneider, Nikolai Maximenko, and Konstantin Lebedev. 2010. "Observational Evidence for Propagation of Decadal Spiciness Anomalies in the North Pacific." *Geophysical Research Letters* 37 (7): n/a-n/a. doi:10.1029/2010GL042716.

Sun, Qiwei, Yan Du, Yuhong Zhang, Ming Feng, Jasti S Chowdary, Jianwei Chi, Shuang Qiu, and Weidong Yu. 2019. "Evolution of Sea Surface Salinity Anomalies in the Southwestern Tropical Indian Ocean During 2010–2011 Influenced by a Negative IOD Event." *Journal of Geophysical Research: Oceans* 124 (5): 3428–3445. doi:10.1029/2018JC014580.

Taguchi, Bunmei, and Niklas Schneider. 2014. "Origin of Decadal-Scale, Eastward-Propagating Heat Content Anomalies in the North Pacific*." *Journal of Climate* 27 (20). Boston MA, USA: American Meteorological Society: 7568–7586. doi:10.1175/JCLI-D-13-00102.1.

Xie, Shang-Ping, and James A. Carton. 2013. "Tropical Atlantic Variability: Patterns, Mechanisms, and Impacts." In *Geophysical Monograph Series*, 147:121–142. doi:10.1029/147GM07.

Zebiak, Stephen E. 1993. "Air-Sea Interaction in the Equatorial Atlantic Region." *Journal of Climate* 6 (8). Boston MA, USA: American Meteorological Society: 1567–1586. doi:10.1175/1520-0442(1993)006<1567:AIITEA>2.0.CO;2.